

Self-assembly of Janus Cyclodextrins at the Air–Water Interface and in Organic Solvents

Bertrand Hamelin,^[a] Ludovic Jullien,^{*[a]} André Laschewsky,^[b] and Catherine Hervé du Penhoat^[c]

Abstract: The self-organization of various amphiphilic cyclodextrins is reported at the air–water interface as well as in organic solvents. These rather rigid molecules expose different molecular surfaces to the external medium according to the nature of the environment, and consequently several types of association are observed. At the air–water interface, stable mono- and multilayers

are formed whose behavior can be related to the molecular structure of the amphiphilic compounds. In apolar aromatic solvents, such as benzene or toluene, dimerization occurs as shown

Keywords: cyclodextrins • hydrogen bonds • monolayers • self-assembly • structural elucidation

by vapour pressure osmometry (VPO), ¹H NMR spectroscopy and ¹H¹³C heteronuclear NOE measurements. Such a feature is absent in organic solvents that compete for the formation of hydrogen bonds. The consequences of these results concerning the use of cyclodextrin derivatives as calibration standards for the determination of molecular weights are discussed.

Introduction

Several natural molecular systems adopt well-defined structures both in hydrophilic and hydrophobic media i) by exposition of favorable groups to the surroundings and ii) by internalization of the poorly interacting structural elements in the core of their structure.^[1] Hence, the conformational translocations of various water-soluble proteins make them able to almost freely cross biological membranes or form channels through lipid bilayers. The structural requirement to observe such a behavior lies in a balanced amount and spatial distribution of the hydrophobic and hydrophilic amino acid residues along proteic secondary structures; the residues of a given type have to be more or less located on the same face. We have been interested in the examination of whether a similar behavior can be observed for large structural segments other than those present in proteins, such as α helices. The basic idea was to prepare cylindrical molecules with a


hydrophobic face and a hydrophilic face (for such molecules, the term Janus was coined^[2]) and to study their aggregation under different medium conditions. Intuitively, one should expect such molecules to dimerize in water or in organic solvents in a way similar to amphiphilic molecules in water, but with a much better control over the stoichiometry of associated species (Figure 1). Cyclodextrins form a class of suitable molecular skeletons for the present purpose. These naturally occurring large molecules are rigid toroids bearing numerous hydroxylic groups that can be facially derivatized to introduce hydrophobic groups.^[3] This provides Janus-type cylinders.

In contrast to the preceding aspect, we have been also concerned with the use of cyclodextrin derivatives as calibration species. For polymers of moderate molecular weights or for self-organized assemblies, many of the methods for determining average molecular weights depend on hydrodynamic experiments (GPC, QELS, viscosity, and so on) or on analysis of colligative properties (osmometry, tonometry, and so on).^[4] Most often, data analysis requires suitable calibrations involving standards whose molecular masses and shapes are known. The preparation and purification of monodisperse polymer standards of precise molecular weights are quite tedious. Consequently, the controlled functionalization of large organic substrates of given molecular weight offers an alternative to afford suitable calibrating standards of molecular weights between 10³ and 10⁴. Ideally, a good standard should be chemically stable, easily purified, soluble in many solvents, and should have a well-defined conformation. Cyclodextrins can easily satisfy these demands, and are therefore highly attractive.

[a] Dr L. Jullien, Dipl. B. Hamelin
Département de Chimie (URA 1679) Ecole normale supérieure
24, rue Lhomond, F-75231 Paris Cedex 05 (France)
Fax: (+ 33) 1-44-32-33-25
E-mail: ludovic.jullien@ens.fr

[b] Prof. Dr. A. Laschewsky
Département de Chimie, Université Catholique de Louvain
Place L. Pasteur, 1, B-1348 Louvain-la-Neuve (Belgium)

[c] Dr. C. Hervé du Penhoat
CERMAV, Domaine Universitaire, 601, rue de la chimie, BP 53
F-38041 Grenoble Cedex 9 (France)

 Supporting information for this contribution is available on the WWW under <http://www.wiley-vch.de/home/chemistry/>

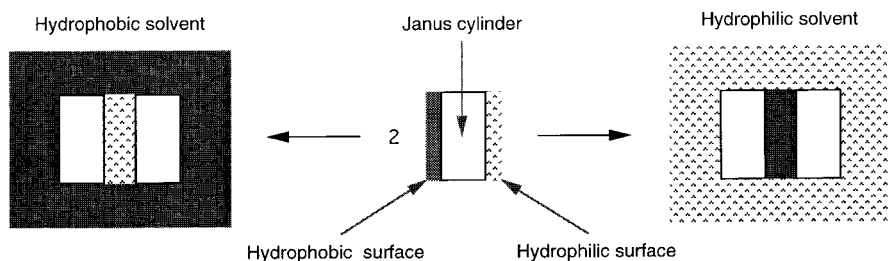


Figure 1. Expected dimerization behavior of Janus-like molecular cylinders towards hydrophilic or hydrophobic solvents.

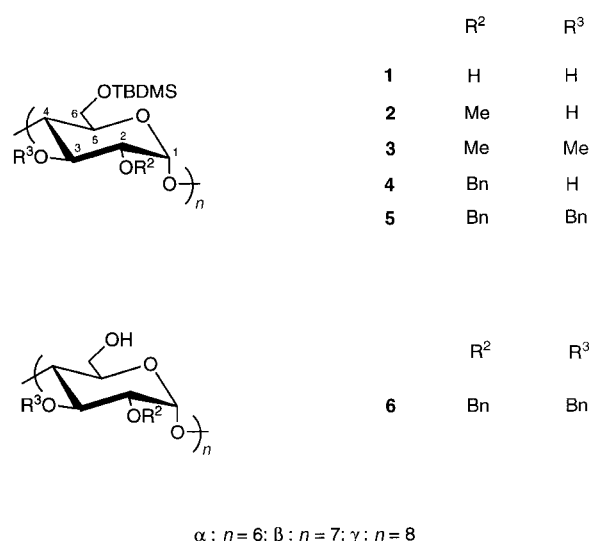
Among cyclodextrin derivatives, the 6-per-(*tert*-butyldimethylsiloxy)cyclodextrins exhibit excellent properties for the applications that have been evoked in the previous paragraphs. These derivatives are easily prepared in one step from the commercially available native cyclodextrins. They can be purified by repeated recrystallisation. Moreover, due to the lack of conformational flexibility, they are expected to exhibit a well-defined mushroom shape. In the present paper, the supramolecular structures resulting from the interaction of various β -cyclodextrin derivatives with water or with several organic solvents are reported and analyzed with regard to the detailed molecular structures.

Results

Synthesis: Two different series of Janus cylindrical molecules were investigated. In the first series (Janus I), the primary face is made hydrophobic by the functionalization of all open sites with *tert*-butyldimethylsilyl groups, whereas symmetrically distributed hydroxyl groups of the secondary face remain underivatized. Thus, the per-6-*tert*-butyldimethylsilyl α -, β - and γ -cyclodextrins **1a**, **1b**, and **1c** bearing 12, 14 and 16 OH groups on the secondary rim, respectively, were obtained following an established procedure (Scheme 1).^[5a] The per-2-methyl **2b**^[5b] and per-2-benzyl **4b** derivatives of **1b** were prepared additionally by alkylation with the corresponding

halogenated compounds by the use of barium oxide/barium hydroxide. The latter molecules contain seven OH groups (Scheme 1). To analyze the Janus behavior, several functionalized β -cyclodextrins derived from **1b** that lack the capacity to make hydrogen bonds were synthesized (Scheme 1). Hence the per-2,3-methyl **3b**^[5b] and per-2,3-benzyl **5b**^[5a] derivatives

have been prepared by alkylation of **1b** by the use of sodium hydride as a base. The second series of Janus molecules (Janus II) results from the functionalization of all open sites of the secondary cyclodextrin face by benzyl groups, while the primary face now bears hydroxyl groups. Cyclodextrins **6b** and **6c** were prepared as previously described.^[5a]



Scheme 1. Numbering scheme for compounds **1–6**.

Behavior of Janus cyclodextrins towards hydroxylic solvents: Compounds **1a**, **1b** and **1c**, with a hydrophobic primary face, and compounds **6b** and **6c**, with a hydrophobic secondary face, barely dissolve in hydroxylic solvents. None of these molecules are soluble in water (*vide infra*)^[6] or in cold methanol or cold ethanol. However, they are soluble in hot methanol and ethanol, which can be used for recrystallisation. In view of these findings, which preclude the study of self-organization in bulk hydroxylic media, the behavior of the amphiphilic cylinders in monomolecular films at the air–water interface was investigated. Both series **1** and **6** give stable Langmuir films whose characteristics are summarized in Table 1. The isotherms are exemplified in Figure 2 at 292 K. Both amphiphilic cyclodextrin series **1** and **6** exhibit very similar behavior (with some minor differences): first, a steep increase of pressure occurs at molecular areas *A* that are close to the expected values when the hydrophilic face of the cylinders is oriented towards water (compare for instance the **1b** values; $A_{01}(\mathbf{1b}) = 340 \text{ \AA}^2$, whereas 320 \AA^2 is the estimate that is based on a **1b** structure generated from Quanta[®]).^[7]

Abstract in French: Cet article présente les structures résultant de l'auto-organisation de cyclodextrines amphiphiles à l'interface eau-air ou en solvant organique. Selon la nature de leur environnement, ces molécules assimilables à des palets rigides exposent différentes faces et donnent ainsi lieu à des modes d'organisation variés. À l'interface eau-air, on observe la formation de mono- et de multicouches dont le comportement s'interprète par la structure de l'amphiphile considéré. Dans les solvants aromatiques apolaires tels que le benzène ou le toluène, il se produit parfois une dimérisation qui peut être mise en évidence par osmométrie, RMN du proton et par des mesures de NOE hétéronucléaire proton-carbone. Lorsque le solvant organique est un compétiteur vis-à-vis de la liaison hydrogène, aucune dimérisation n'est observée. Les résultats obtenus sont analysés à la lumière de l'utilisation de dérivés de cyclodextrines comme étalons de calibration pour la détermination de masse moléculaire.

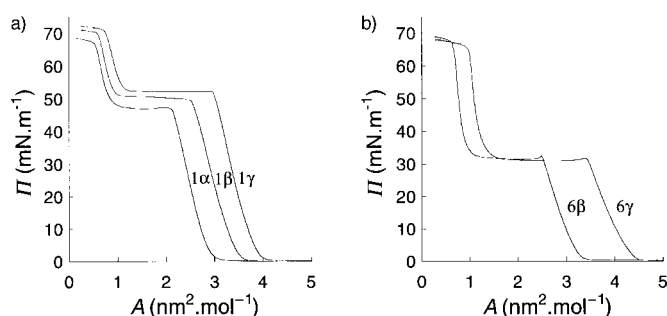


Figure 2. Surface-pressure isotherms of **1** (a) and **6** (b) at the air–water interface at 292 K. Compression rates: $0.5 \text{ \AA}^2 \text{ s}^{-1} \text{ molecule}^{-1}$ (**1α**); $0.9 \text{ \AA}^2 \text{ s}^{-1} \text{ molecule}^{-1}$ (**1β**); $0.7 \text{ \AA}^2 \text{ s}^{-1} \text{ molecule}^{-1}$ (**1γ**); $0.6 \text{ \AA}^2 \text{ s}^{-1} \text{ molecule}^{-1}$ (**6β** and **6γ**).

Table 1. Structural and thermodynamic parameters at 292 K as extracted from Langmuir isotherms of the cyclodextrin derivatives **1α**, **1β**, **1γ**, **6β**, and **6γ** (see Experimental Section).

	$A_{01}^{[a]}$	$A_c^{[b]}$	$\Pi_c^{[c]}$	$\Delta A_c^{[d]}$	$A_{02}^{[e]}$	A_{01}/A_{02}	$W^{[f]}$	$\Delta H^0^{[g]}$	$10^3 \kappa^{[h]}$
1α	285	215	47.1	135	145	2.0	40	(−20)	6.0
1β	340	255	50.5	165	160	2.1	55	(−30)	5.8
1γ	380	300	52.4	190	190	2.0	60	(−55)	4.6
6β	320	250	31.2	160	110	2.9	40	−77	9.5
6γ	425	345	31.7	225	145	2.9	54	−56	8.0

[a] Molecular surface in \AA^2 as extrapolated to $=0 \text{ mN m}^{-1}$ from the slope of the experimental isotherm just before the first collapse. [b] Molecular surface in \AA^2 at the first collapse. [c] Pressure of the first collapse in mN m^{-1} . [d] Plateau width at Π_c in \AA^2 . It is obtained by subtracting from A_c the abscissa of the intercept of the slope of the experimental isotherm just before the second collapse with the plateau at Π_c . [e] Molecular surface in \AA^2 as extrapolated to $=0 \text{ mN m}^{-1}$ from the slope of the experimental isotherm just before the second collapse. [f] Compression work that is received when the molecular surface is reduced by ΔA_c at the pressure Π_c in kJ mol^{-1} . [g] Reaction enthalpy for the first collapse process as obtained from the Clapeyron Equation (1) in kJ mol^{-1} . The values for **1α**–**γ** are given in brackets since the compressions were not performed under quasistatic conditions for this series of cyclodextrin derivatives (see text). [h] Isothermal compressibility at $\Pi_c/2$ in mN m^{-1} [$\kappa = -(1/A)(\partial A/\partial \Pi)_T$].

Plateaus at moderate surface pressures of about 30 mN m^{-1} in the case of series **6**, and at high surface pressures of about 50 mN m^{-1} in the case of series **1** are then observed. Upon further compression, the surface pressures increase once more, the rise in surface-pressure being terminated by a collapse at maximal surface pressures of about 70 mN m^{-1} . Within each series, analogous trends between the α -, β -, and γ -cyclodextrin derivatives are observed. For the compounds **1**, which are silylated on the primary face, both molecular area A_{01} and plateau pressure Π_c steadily increase when going from homologues α to γ , whereas the monolayer compressibility (κ) decreases. However, the plateau surface pressures Π_c for **6β** and **6γ**, which are benzylated on the secondary face, are identical, but the molecular surface A_{01} increases when going from the β to γ homologue. As found for the series **1**, the monolayer compressibility κ decreases from β to γ . Another difference between the Langmuir films of series **1** and **6** concerns the ratio between the molecular areas at the first increase and at the second increase of the surface pressure (A_{01}/A_{02}). A_{01}/A_{02} is about two for series **1**, but is about three for series **6**.

To estimate the relevance of the present experiments for the derivation of thermodynamical data, compression–expansion cycles were performed for **1γ** and **6γ** at several compression rates. A pronounced hysteresis for molecular area was observed for **1γ**, suggesting that the isotherms in the **1** series were recorded under kinetic control (Figure 3a). In

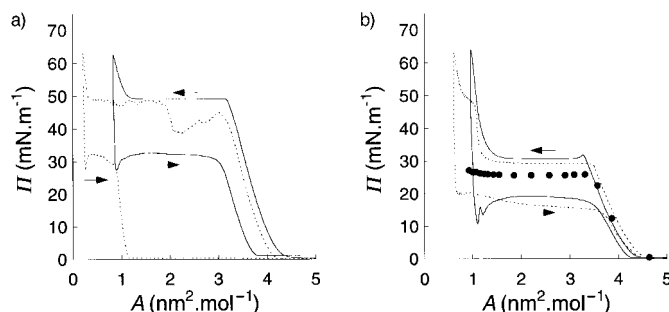


Figure 3. Compression–expansion cycles for **1γ** (a; 301 K; continuous line: 1.4–15–1.4, broken line: 0.2–15–0.2) and for **6γ** (b; continuous line: 292 K, 0.6–15–0.6, broken line: 301 K, 0.1–15–0.1). The black circles were obtained during the spreading experiment that was done at constant trough area; see text) at the air–water interface. In the notation x – y – x , x is the compression and expansion rate expressed in $\text{\AA}^2 \text{ s}^{-1} \text{ molecule}^{-1}$ and y is the delay (in minutes) during which the pressure has been maintained at 63 mN m^{-1} .

contrast, **6γ** displayed only a small hysteresis of molecular area (Figure 3b) at the compression rate that was typically applied to measure the surface-pressure isotherms that are presented on Figures 2 and 4. In a further experiment, increasing numbers of drops of **6γ** solution were dispersed over the Langmuir trough at constant area (black circles on Figure 3b). At very high molecular areas ($A > 5 \text{ nm}^2 \text{ mol}^{-1}$), the drop rapidly evaporates. The evaporation process takes about one second in the regime of pressure increase ($3.5 \text{ nm}^2 \text{ mol}^{-1} < A < 4.5 \text{ nm}^2 \text{ mol}^{-1}$). This delay is increased to thirty seconds at the plateau ($A < 3 \text{ nm}^2 \text{ mol}^{-1}$), where visible amounts of solid are left by solvent evaporation, thus providing a three dimensional reservoir of **6γ** in stable thermodynamic equilibrium with the monolayer. This experiment provides an extrapolated A_{01} molecular area and a plateau value Π_c that are very similar to those displayed in Table 1. Both observations suggested that the isotherms in the **6** series were recorded close to equilibrium conditions. For the thermodynamic treatment of the monolayer data, the external work W corresponding to the compression at Π_c along the plateau width ΔA_c was first derived. It corresponds to the Gibbs free energy ΔG^0 of the transition for a quasistatic transformation. For both series **1** and **6**, this work increases when going from homologue α to γ (Table 1). To evaluate the enthalpy of the transition, isotherms of series **1** and **6** were recorded at several temperatures.

The isotherms are only slightly temperature sensitive in series **1** (Figure 4a). However, they are notably affected in series **6**, the plateau pressure decreasing with increasing temperature. One also notices the emergence of a second plateau at temperatures above 301 K (Figure 4b). The ratio of A_{01} to the corresponding molecular surface A_{03} is about 4–5 for both **6β** and **6γ**. The enthalpy ΔH^0 associated with the first

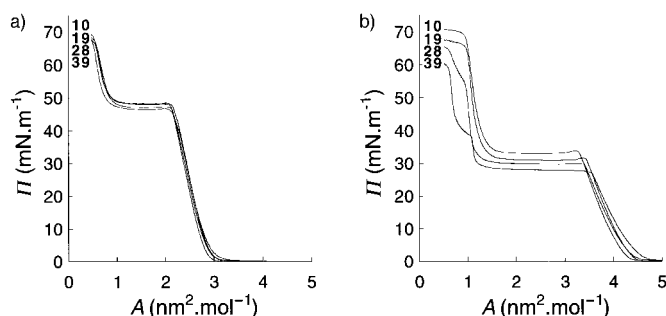


Figure 4. Surface-pressure isotherms of **1α** (a) and **6γ** (b) at the air–water interface as a function of temperature (given on the figure in °C). Compression rates: $0.5 \text{ \AA}^2 \text{ s}^{-1} \text{ molecule}^{-1}$ (**1α**); $0.6 \text{ \AA}^2 \text{ s}^{-1} \text{ molecule}^{-1}$ (**6γ**).

collapse can be obtained at thermodynamic equilibrium from the Clapeyron equation [Eq. (1)].^[8] The Clapeyron equation gives the relation between ΔH^0 , the collapse pressure Π_c , and the plateau width ΔA_c . Thus $\Delta H^0(\mathbf{6}\beta)$ and $\Delta H^0(\mathbf{6}\gamma)$ can be derived (Table 1), showing that $\Delta H^0(\mathbf{6}\beta)$ is more negative than $\Delta H^0(\mathbf{6}\gamma)$.

$$\frac{d\Pi_c}{dT} = \frac{\Delta H^0}{T\Delta A_c} \quad (1)$$

Behavior of Janus cyclodextrins towards hydrophobic sol-

vents: In view of the purpose to use the present cyclodextrin derivatives as calibrating species for determination of molecular weights, the attention was focused on typical solvents used for such analyses. Thus the eventual aggregation of the cyclodextrin samples was investigated in toluene, chloroform, and THF.

In a first series of experiments, the determination of average molecular weights have been performed in toluene by vapour pressure osmometry (VPO) experiments. These experiments were made in the concentration range 1–50 mM. Very good linear signal–concentration relationships were observed for the **1–6β** β-cyclodextrin derivatives in this range (Scheme 1). The extrapolated signals at zero concentration have been converted into molecular weights after calibration with monodisperse polystyrene samples. Table 2 sums up the experimental observations.

Whereas the experimentally determined average molecular weights by number MW_{VPO} are in satisfying agreement with the theoretical expectations MW_{theory} for **2–5β**, a strong deviation is observed for **1β**. $MW_{VPO}(\mathbf{1}\beta)$ is virtually twice the

Table 2. Number average molecular weights of β-cyclodextrin derivatives as determined by VPO experiments in toluene (see experimental section).

Molecular formula	Theoretical molecular weight MW_{theory}	Experimental molecular weight $MW_{VPO}(\pm)$	MW_{VPO}/MW_{theory}
1β ($C_{12}H_{24}O_5Si_7$)	1934.87	3970 ^[a]	2.05
2β ($C_{13}H_{26}O_5Si_7$)	2033.08	2050	1.01
3β ($C_{14}H_{28}O_5Si_7$)	2131.22	2160	1.01
4β ($C_{15}H_{30}O_5Si_7$)	2565.78	2520	0.98
5β ($C_{26}H_{36}O_5Si_7$)	3196.62	2660	0.83
6β ($C_{20}H_{22}O_5Si_7$)	2396.73	2585	1.08

[a] Based on 4 independent determinations.

value of $MW_{theory}(\mathbf{1}\beta)$. This observation suggests that **1β** spontaneously dimerizes in toluene solutions at room temperature, even at as low concentrations as 1.5 mM.

To analyze the exceptional behavior of **1β**, a series of ¹H NMR spectroscopic experiments was conducted in deuterated benzene, to evidence any modification of NMR signals that should occur on changing the **1β** concentration. Under appropriate conditions, the thermodynamic description of an associated species (stoichiometry, stability) can be derived from a titration experiment (e.g., recording ¹H NMR spectra as a function of **1β** concentration in the present case).^[9] Since the VPO experiment suggested that the apparent composition of the solution remains stable as a function of concentration in the accessible concentration range for ¹H NMR at room temperature, the behavior of the ¹H NMR spectrum of **1β** as a function of the temperature was first examined to determine i) the most sensitive signals; ii) the most favourable temperature range to perform the titration experiment. Figure 5 displays the evolution of the **1β** chemical shifts as a function of temperature in a 0.21 mM C_6D_6 solution together with some representative chemical shifts of the model compounds **2β** and **3β** at the same concentration at 293 K.

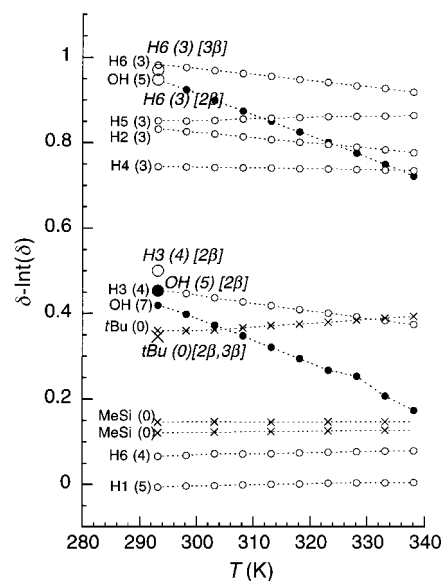


Figure 5. Evolution of **1β** chemical shifts as a function of temperature (0.21 mM **1β** solution in C_6D_6). The corresponding chemical shifts for the model compounds **2β** and **3β** at the same concentration at 293 K are shown as large circles and crosses. Chemical shifts on the y axis are given as the difference between the actual value of the chemical shift and the inferior (i.e., rounded down) integer which is given in brackets for each attributed signal.

At room temperature, the chemical shifts of **1β**, **2β**, and **3β** are essentially identical as expected from the close structures of the parent compounds. Interestingly, the **2β** 3-hydroxyl group is considerably shifted (–0.5 ppm) with regards to the corresponding **1β** signal. Rotamer populations have been extracted from the $^3J_{5,6a}^{exp}$ and $^3J_{5,6b}^{exp}$ vicinal coupling constants at 298 K for **1β**, **2β**, and **3β** (see Experimental Section). Upon considering only the three staggered conformers *gauche*, *gau-*

che (GG), *gauche,trans* (GT), and *trans,gauche* (TG), simulations indicate a 0.4:0.6 GG:GT average for **1β** (${}^3J_{5,6a}^{\text{exp}} = 3.1$ Hz and ${}^3J_{5,6b}^{\text{exp}} = 7.1$ Hz), a 0.4:0.6 GG:GT average for **2β** (${}^3J_{5,6a}^{\text{exp}} = 3.0$ Hz and ${}^3J_{5,6b}^{\text{exp}} = 7.1$ Hz), and a 0.6:0.4 GG:GT average for **3β** (${}^3J_{5,6a}^{\text{exp}} = 2.3$ Hz and ${}^3J_{5,6b}^{\text{exp}} = 5.2$ Hz). The influence of temperature on **1β** chemical shift is rather weak; the **1β** hydroxyl signals and the signal of the proton at the 3-glucose position are the most affected by changing temperature. The **1β** 3-hydroxyl ${}^1\text{H}$ NMR signal is shifted towards the corresponding chemical shift of the reference compound **2β** when the temperature is increased.^[10] By assuming that the changes of chemical shifts were governed by the modification of the position of the monomer–dimer equilibrium, a titration experiment was performed at 320 K in the 0.1–10 mM concentration range. We aimed at forming significant amounts of monomer at low concentrations, while keeping enough signal intensity for ${}^1\text{H}$ NMR.

Figure 6a displays the results for the chemical shifts measured. It shows that they are almost insensitive to the concentration of **1β** in the investigated range. In fact, only the protons of the *tert*-butyl group are affected, essentially beyond 2 mM where the evolution is linear. Such a linear behavior cannot be accounted for if we assume the equilibrium given in Equation (2) takes place, as in this concentration range the anticipated curve should show a convex shape. Equation (3) describes the average chemical shift in the fast exchange regime.

$$2\mathbf{1}\beta = (\mathbf{1}\beta)_2 \quad (2)$$

$$\delta([1\beta]_{\text{tot}}) = \delta_{(1\beta)_2} + (\delta_{1\beta} - \delta_{(1\beta)_2}) \left[\frac{-1 + \sqrt{1 + K[1\beta]_{\text{tot}}}}{4K[1\beta]_{\text{tot}}} \right] \quad (3)$$

No satisfactory fit can be found according to the corresponding law given in Equation (3) with $\delta_{1\beta} = \delta([1\beta]_{\text{tot}} \rightarrow 0) = 0.378$ (experimental value), in which the equilibrium constant K and the intrinsic chemical shift $\delta_{(1\beta)_2}$ of the *tert*-butyl signal

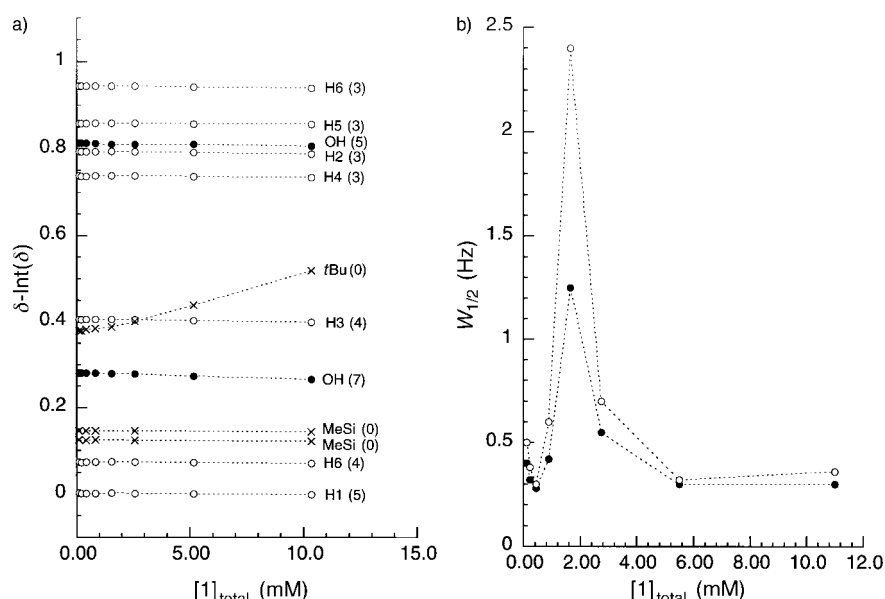


Figure 6. Evolution of **1β** a) chemical shifts and b) widths at half-height of the hydroxyl signals as a function of the **1β** concentration ($T = 320$ K). On Figure 6a, chemical shifts on the y axis are given as the difference between the actual value of the chemical shift and the inferior integer which is given in brackets for each attributed signal.

in $(\mathbf{1}\beta)_2$ are taken as floating parameters. In contrast, the drift of the signal of the *tert*-butyl group beyond 2 mM can be explained by considering that one moves from a diluted to a concentrated regime of concentration; below such a value, the solution is diluted and whatever the concentration $[1\beta]_{\text{tot}}$, the environment of **1β** does not change. However, **1β** molecules start to considerably see each other above 2 mM so as to modify the average **1β** chemical shift.^[11] In the course of this titration experiment, a significant broadening of the hydroxyl signals around 2 mM has been also noticed (Figure 6b). Although this observation suggests a change of regime for chemical exchange between the monomeric and the dimeric **1β** states, it cannot be easily analyzed in view of the too large number of unknown thermodynamic, kinetic, and spectroscopic parameters.

To complete the preceding series of ${}^1\text{H}$ NMR experiments, dynamic ${}^{13}\text{C}$ NMR experiments were performed to shed light on the hydrodynamic features of the associated species derived from **1β**. Such NMR experiments provide experimental data that can be compared with simulated values resulting from the knowledge of molecular structures and tumbling motion.^[12] Cyclodextrin substrates are suitable substrates for such analysis. They are known to have a rather rigid skeleton and can be reasonably considered as rigid bodies for the hydrodynamic analysis. Moreover, their symmetrical shape simplifies the description of the tumbling motion. In this work, the heteronuclear proton–carbon NOE factors (NOEF; η) for the six (C,H) couples borne by the glucose units contained in the cyclodextrin skeleton of **1β** and **3β** have been experimentally measured for the present purpose.^[13] The results are displayed on Table 3. Since the NOEF are decreasing functions of the molecular friction, the lower values that are observed for **1β** confirmed that this compound aggregates in benzene solution.

In order to analyze the origin of the interaction between **1β** molecular units, complementary experiments were made

either by trying to directly evidence hydrogen bonding or by analyzing the association behavior in different solvents that were expected to compete for the hydrogen-bonding interaction. IR absorption spectra were first recorded. The IR spectrum of the solid **1β** in KBr exhibits a broad absorption band corresponding to OH stretching that is centered at 3395 cm^{-1} . In contrast, a concentrated solution of **1β** in mesitylene displays two absorption bands at 3429 and 3294 cm^{-1} . Then size exclusion chromatography (SEC) was performed in different solvents for **1–3β**.^[14] Calibration of molecular weights has been performed with the same polystyrene samples as for VPO experiments.

Table 3. Experimental NOE factors (NOEF) $\eta(i)$ for the six (C,H) couples borne by the cyclodextrin backbone of the compounds **1 β** (2.1×10^{-2} M in [D₆]benzene) and **3 β** (1.9×10^{-2} M in [D₆]benzene). The numbering of atom positions is given on Scheme 1. The $\eta(i)$ values are given with a precision equal to 10 %.

	$\eta(1)$	$\eta(2)$	$\eta(3)$	$\eta(4)$	$\eta(5)$	$\eta(6)$	$\langle\eta\rangle(1-5)$
1β	0.41	0.39	0.39	0.39	0.40	0.40	0.40
3β	0.96	0.94	0.94	0.94	0.96	1.04	0.95

Table 4 summarizes the results. Unfortunately, **1 β** irreversibly adsorbs on the styragel column in toluene and SEC experiments were not pursued in this solvent. In THF the apparent molecular weight is close to the expected value, whatever the compound. The analysis of the position and the

Table 4. Average molecular weights of **1 β** , **2 β** and **3 β** as determined by SEC experiments in several solvents.

	Experimental molecular weight MW _{GPC} ($\pm 10\%$)	Poly-dispersity	MW _{GPC} /MW _{Theory}
1β (toluene)	– ^[a]	–	–
1β (chloroform)	2290	1.04	1.18
1β (THF)	1910	1.03	0.99
2β (chloroform)	1450	1.04	0.71
2β (THF)	1840	1.06	0.91
3β (chloroform)	1590	1.04	0.75
3β (THF)	1990	1.02	0.93

[a] Irreversible adsorption on the column.

shape of SEC chromatograms resulting from dynamic exchange between species in equilibrium is rather difficult.^[15] The observation of only one peak suggests either i) the existence of a predominating species in a slowly exchanging mixture,^[16] or ii) a fast exchange regime with a peak position related to the positions and the relative proportions of exchanging species. Whatever the situation, the observation of a single SEC peak at an apparent molecular weight that corresponds to the monomeric form suggests that **1 β** essentially exists as a monomer in THF. The chloroform results are more surprising. Indeed the experimentally observed molecular weights for **2 β** and **3 β** are lower than the theoretical ones. This is in line with the better solvent character of chloroform for swelling the polystyrene calibrating samples. In contrast, the experimental value for **1 β** is too large. From this sole experiment, it could be deduced that **1 β** partially dimerizes in chloroform in a fast exchange regime. As suggested by complementary NMR spectroscopic experiments (vide infra), this result is better explained by considering that the **1 β** hydrodynamic volume is reasonably larger than for **2 β** and **3 β** in view of the capability of **1 β** to form stronger bonds with

chloroform. To complete the SEC observations, **1 β** ¹H NMR spectra were recorded at 0.1 mm and 1 mm in deuterated chloroform and deuterated acetone. No significant change of chemical shifts was observed between both concentrations. Hence, even at high concentration, no aggregation is observed in those solvents. Table 5 compares the chemical shifts of all protons in the deuterated benzene with those in acetone and chloroform at the same concentration of **1 β** . It is interesting to note that the difference in chemical shift in deuterated benzene and in the other solvents is significantly more pronounced for the protons borne on the secondary cyclodextrin face.

Discussion

Behavior of Janus cyclodextrins at the air–water interface:

The Janus cyclodextrins **1 α** – γ and **6 β** – γ produce stable Langmuir films at the air–water interface.^[17] As for other reported cyclodextrin derivatives,^[18–22] their surface pressure isotherm is close to that of rather rigid amphiphilic discs. At large molecular areas, solid-analogous islands in a gas-analogous matrix occur. A sudden increase of surface pressure takes place when the islands start to touch. At the collapse pressure, some molecules contained in the monolayer are pushed up, and a three-dimensional structure is formed besides the monolayer at the air–water interface. Such a picture, supported by the molecular areas A_{01} that can be extracted from extrapolation of the isotherms at the collapse, points to a surface pressure equal to zero. If we assume that these molecules adopt a compact hexagonal two-dimensional structure at the collapse (compactness = 91 %), the molecular radii of **1 α** , **1 β** , and **1 γ** are 0.9 nm, 1.0 nm, 1.05 nm, respectively, and those of **6 β** and **6 γ** are 0.95 nm and 1.1 nm, respectively. These radii do not directly compare with the external radii of the native cyclodextrins, which are 0.73 nm, 0.77 nm and 0.87 nm for the α -, β - and γ -cyclodextrins, respectively. The differences suggest that the hydrophobic parts of the derivatized cyclodextrins determine the area that is occupied at the air–water interface. This interpretation is corroborated by the observation of the Quanta molecular models that indicate a mushroom shape whose external diameter increases slightly when going from α -cyclodextrins to γ -cyclodextrins. The compressibility κ associated with the formation of a dense monolayer is thus rationalized in terms of the packing of the hydrophobic part. In average, the steric hindrance promotes a larger exposure of the hydrophobic residues to the exterior of the structure for the smaller cyclodextrins. As a consequence, the relative variation of the molecular area from a loose contact to a densely packed state

Table 5. Chemical shifts δ of **1 β** in deuterated benzene, deuterated acetone and deuterated chloroform at 294 K and 0.21 mm. For numbering, see Scheme 1.

	OH _a	OH _b	H ₁	H ₂	H ₃	H ₄	H ₅	H _{6a}	H _{6b}	<i>t</i> Bu	Me _a Si	Me _b Si
δ [C ₆ D ₆]	7.42	5.95	4.99	3.83	4.45	3.74	3.85	4.07	3.98	0.36	0.15	0.12
δ [CDCl ₃]	6.68	5.21	4.83	3.59	3.98	3.50	3.57	3.84	3.65	0.81	–0.02	–0.03
δ [(CD ₃) ₂ CO]	5.58	5.12	4.92	3.404	3.85	3.55	3.71	4.04	3.78	0.87	0.06	0.05
δ [CDCl ₃]- δ [C ₆ D ₆]	0.74	0.73	–0.16	–0.25	0.48	–0.24	–0.28	–0.23	–0.33	0.45	–0.17	–0.15
δ [(CD ₃) ₂ CO]- δ [C ₆ D ₆]	1.84	0.83	–0.08	0.43	0.60	–0.19	–0.14	–0.03	–0.21	0.51	–0.08	–0.07

(or the compressibility κ) is larger for the smaller cyclodextrins. This effect is more pronounced for series **6** because the hydrophobic residues (benzyl groups in this case) are more numerous and are individually less rigid than the *tert*-butyl groups of series **1**.

A remarkable feature of the isotherms of all the studied Janus cyclodextrins is the presence of two and even three (see Figure 3b at 28 °C and 41 °C) successive steep increases of pressure when the molecular area is reduced. Such a behavior has been already reported in the past for amphiphilic cyclodextrins^[17, 21, 23] and for other molecules.^[24] It is generally interpreted as resulting from the formation of multilayer structures. Assuming that the Langmuir film at the air–water interface is homogeneous, the number of molecular layers at a given surface pressure can be calculated by dividing the molecular area at the first collapse A_{01} by the molecular area at the second A_{02} or the third A_{03} , when the latter exists. In the present series of cyclodextrins, numbers that are close to integer values are obtained (Table 1). In the series **1** $A_{01}/A_{02} \approx 2$, whereas $A_{01}/A_{02} \approx 3$ and $A_{01}/A_{03} \approx 4-5$ for series **6**.

The formation of bilayers in series **1** would be rather unusual. In fact the hysteresis experiments and some preliminary AFM observations on transferred films suggest that beyond the collapse point, films of **1 α – γ** are rather heterogeneous and contain small three-dimensional crystals. The formation of trilayers in the case of **6 β** and **6 γ** is consistent with a previous report on transferred azido cyclodextrins, which clearly imaged trilayers and other types of layering at the molecular level^[25a] and with the general trend that is observed for more classical amphiphilic molecules.^[25b] AFM pictures suggest that the films of **6 β** and **6 γ** , which are transferred at the plateau pressure Π_c , are homogeneous with large smooth zones separated by discrete steps. These differences in the behavior of series **1** and **6** are in line with the respective structures of these molecules. A stronger cohesion of the hydrophobic contact in the liquid trilayer is expected for series **6** as opposed to series **1**, since interdigitation without crystallisation are easiest in the former series (weaker stiffness and smaller steric hindrance). For series **6**, the plateau at Π_c appears to correspond to the equilibrium domain between the monolayer and the trilayer state. It is interesting to notice that the standard reaction enthalpy for the formation of the trilayer is negative, whereas the corresponding standard Gibbs free energy is positive (W in Table 1). Hence, entropy seems to strongly disfavour the process of building trilayers.

In conclusion, the homo-association between hydrophobic faces of Janus cylinders is promoted at the air–water interface, but is revealed in different ways according to the cohesion of the three-dimensional crystals. In the case of the soft Janus II cylinders, the air–water interface exerts a rather long-range orienting effect that is reflected by the formation of homogeneous mono-, tri-, or even multilayers of higher order at thermodynamic equilibrium. In contrast, when the lattice energy of the three-dimensional crystals of Janus cylinders is large enough, so that it can compete efficiently with the water-organizing effect to determine the molecular organization at the air–water interface, heterogeneous metastable structures are formed.

Behavior of Janus cyclodextrins in apolar aromatic solvents:

The VPO experiments show that **1 β** exhibits a particular aggregation behavior in toluene with regards to the other β -cyclodextrin derivatives investigated. It spontaneously dimerizes at concentrations as low as 1 mM. In view of the strong similarity between benzene and toluene as well as from the results extracted from relaxation NMR experiments (vide infra), the absence of evolution of chemical shift during ¹H NMR titrations suggests that the dimerization state remains stable down to concentrations of 0.1 mM in benzene. These observations provide an estimate of the equilibrium constant at 320 K for the dimerization process given by Equation (2) in aromatic solvents; K exceeds 5×10^7 . This corresponds to a standard Gibbs free energy of dimerization $\Delta G_{320}^0(\text{dim})$ lower than -47 kJ mol^{-1} . In addition, if one considers that the most sensitive ¹H NMR signal of **1 β** to the change of temperature, the 3-hydroxyl proton, tends towards the behavior of the monomeric model compound **2 β** at high temperature, the dimerization process appears to be disfavored by a temperature increase, thus indicating a corresponding negative standard reaction enthalpy.

The structure of the **1 β** dimer can be first analyzed at a low-level of description from NMR relaxation experiments. It is possible to estimate the volume and the shape of the dimerized species from the treatment of the experimental NOE factors η_{exp} as follows. In a first step, the hydrodynamic radius R in deuterated benzene of the monomeric model compound **3 β** is evaluated by assuming that its tumbling motion is isotropic in view of its rather spherical structure (one correlation time τ_c). NOE factors $\eta_{\text{sim}}^{\text{iso}}(\tau_c)$ were simulated from Equations (8) and (9) and $\tau_c(R)$ values were simulated from Equation (12) [see Experimental Section]. The experimental average value η_{exp} for the five (C,H) couples of the cyclodextrin skeleton is equal to 0.95 (Table 3). This corresponds to a hydrodynamic radius $R = 0.9 \text{ nm}$ ($\eta_{\text{sim}}^{\text{iso}}(0.5 \text{ ns}) = 0.95$ and $\tau_c(0.9 \text{ nm}) = 0.5 \text{ ns}$). This value is in line with the **3 β** structure generated with the MSI molecular modelling package (Quanta®). This fair agreement supports the validity of the hydrodynamic approach to analyze the structures of molecular assemblies based on cyclodextrin skeletons.^[12] In particular, it suggests that the Equation (12) [see Experimental Section] is valid in aromatic solvents at the relevant nanosecond timescale of the present NMR relaxation experiment.^[26] When the same numerical treatment was applied to the data of **1 β** , a hydrodynamic radius equal to 1.2 nm was obtained. Since the structural difference between **1 β** and **3 β** towards solvation with benzene is small, this result suggests that **1 β** aggregated in toluene. Moreover, in view of the **3 β** hydrodynamic radius equal to 0.9 nm, the value of 1.2 nm strongly supports the view that the aggregation of **1 β** is a dimerization process as evidenced by VPO. For a dimer, the assumption of isotropic tumbling is not valid anymore, and different symmetrically axial geometries (ellipsoid, dumbbell, cylinder) whose spectral density functions were available in the literature were considered to account for the structure of the **1 β** dimer (diameter: D , length: L). The tumbling motion is now characterized by two correlation times τ_{\parallel} and τ_{\perp} , corresponding to the reorientation around the symmetry axis and around an axis perpendicular to the symmetry axis,

respectively. For the three envisaged shapes, both the NOE factors $\eta_{\text{sim}}^{\text{aniso}}(\tau_{\parallel}, \tau_{\perp})$ and $[\tau_{\parallel}(L/D), \tau_{\perp}(L/D)]$ couples were simulated from Equations (8), (10), (13), and (14) [see Experimental Section], in order to establish a relation between $\eta_{\text{sim}}^{\text{aniso}}$ and the L/D ratio. Eventually the mean standard deviation F between simulated $\eta_{\text{sim}}^{\text{aniso}}$ and experimental η_{exp} was systematically calculated as a function of L/D . The position of the F minimum gives the length L once the diameter D is known. Upon consideration of the 3β hydrodynamic radius and the larger sterical hindrance at the level of the *tert*-butyl dimethylsilyl groups, and, in addition, if the experimental surface extracted from the surface pressure isotherms at the air–water interface is taken into account, the D value was taken equal to 2.0 nm. Among the three shapes that were investigated, only the cylindrical description provides a pronounced minimum of the F function with $D = 2$ nm (Figure 7).

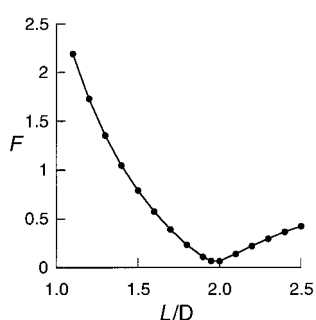


Figure 7. Mean standard deviation F between simulated $\eta_{\text{sim}}^{\text{aniso}}$ (cylinder) and experimental η_{exp} as a function of the ratio L/D where L and D respectively designates the length and the diameter of the 1β dimer (see text and experimental section). D has been taken equal to 2.0 nm.

The F minimum corresponds to a length L equal to 3.9 nm. If evaluating the height (h) of 1β from the Quanta model ($h \approx 1.3$ nm), the distance (d) between both monomeric units in the 1β dimer is about 1.3 nm. In view of the following discussion that suggests a rather tight adhesion between interacting secondary faces in the 1β dimerization process, the latter result appears to be too large. The discrepancy could originate from the underestimation of the friction on the $(1\beta)_2$ dimer with regards to the friction on the 3β monomeric unit. One could imagine the good agreement between the 3β structure and its measured hydrodynamic radius to result from the average over the smooth secondary face and the haired primary face that introduces a larger friction. In the $(1\beta)_2$ dimer where the smooth secondary surface is hidden (vide infra), the friction could be underestimated leading to too large a value of the length L .^[27] As a conclusion from the dynamic NMR experiments, the 1β dimer can be hydrodynamically described as a self-assembled cylinder that results from the association between lateral discoidal faces.

The set of dynamic NMR experiments does not provide any clue concerning the relative orientation of both 1β monomeric units within the dimer. The two different orientations that are compatible with a dimerization process are shown on Figure 8. To address the issue of orientation, the reasoning is based on the fact that external groups i) will give signals that

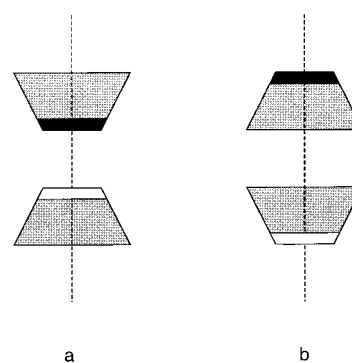


Figure 8. Possible orientations of monomeric units within the 1β dimer. a) primary faces facing together; b) secondary faces facing together.

are strongly environment dependent; these signals should not depend on the monomeric–dimeric state of 1β , and ii) will experience the same environment in 1β and in the model compounds. In striking contrast, the internal groups will be poorly affected by a change of solvent, but be strongly affected when going from a monomeric to a dimeric state. It is noticeable that i) the chemical shifts of the protons borne by the secondary face of 1β are much more temperature sensitive (Figure 5) and affected by a change of the aggregation state (Table 5) than the other signals, ii) the rotameric distribution in toluene is the same for 1β and 2β ;^[28] this suggests that the primary face of 1β is not affected by dimerization, and iii) only the *tert*-butyldimethylsilyl groups experience the change of concentration regime for chemical shift above 2 mM. All these observations indicate that the primary face is external and the secondary face internal in the 1β dimer so as to favor the picture illustrated in Figure 8b.

The origin of the attractive interaction between 1β units in aromatic solvents is now discussed. A first clue is provided by the comparison of the association behavior for the $1-5\beta$ derivatives. Only 1β is able to self-assemble through a hydrogen-bond network linking the interacting secondary faces. 2β and 4β contain hydroxyl groups, but since they are borne at the C3 glucose position, they are supposed to be engaged in an intramolecular hydrogen bond with the oxygen atom borne on the C2 position of the neighbouring glucose unit. Furthermore, due to the presence of a methyl or a benzyl substituent at the C2 glucose position, dimerization is expected to be sterically hindered. The sensitivity of the 1β hydroxyl ^1H NMR signals to the temperature is also in agreement with the direct involvement of the hydroxyl groups in the attractive interaction. In the absence of any suitable reference, the IR absorption spectrum of 1β is only poorly informative, but does not contradict the preceding claim. The absence of 1β dimerization in chloroform, tetrahydrofuran, or acetone seems reasonable, since all these solvents can be expected to solvate 1β through hydrogen bonding and so to inhibit dimerization. Quantitatively, the upper limit of the Gibbs free energy associated with the dimerization of 1β in benzene or toluene is also in agreement with the formation of about seven^[29] hydrogen bonds between the monomeric units (10 kJ mol^{-1} per hydrogen bond^[30]). From this point of view, it is interesting to notice that although they respectively contain seven and eight hydroxyl groups, 6β and 6γ do not dimerize in

toluene, even at concentrations as high as 50 mM. This observation may indicate that the larger mobility of the primary hydroxyl group borne at the C6 glucose position is less favorable to the formation of a hydrogen-bond network. It is also possible that several hydroxyl groups on the primary face are engaged into intramolecular hydrogen bonds. Such an assumption has already been made for explaining abnormal conformational behavior for several α -cyclodextrin derivatives.^[31] Moreover, the latter observation also suggests that the network of hydrogen bonds is directly involved in the dimerization of **1 β** . Indeed, as a result of the presence of some residual water molecules in aromatic solvents, it should be possible to imagine a tiny water pool to link two **1 β** molecules, very much like in inverse micelles.^[32]

Conclusion

The present study illustrates the diversity of association behavior exhibited by rigid Janus molecules under various conditions of media. Despite the balanced structure of the herein reported amphiphilic cylinders, it has been impossible to simultaneously observe a dimerization both in hydroxylic and in hydrophobic media as depicted in Figure 1. A relative flexibility is probably a prerequisite to obtain enough internal mobility to adapt to the different media. Nevertheless, the significance of the respective associating parts of the Janus cyclodextrins that are emphasized on Figure 1 is underlined by the present results. Thus although displaying similar structures, the Janus I and II series display different ways of aggregation at the air–water interface that are thought to be essentially controlled by the hydrophobic core of these amphiphilic molecules. In contrast, in hydrophobic solvents, the association behavior seems now to be governed by the hydrophilic part of the Janus molecules. Hence, in the absence of solvent competition for hydrogen bonding, a stable self-assembled dimer of β -cyclodextrins held by noncovalent interactions was observed in toluene solutions as evidenced by VPO, ¹H, and ¹³C NMR experiments. The comparison of the behavior of related compounds in several solvents under different experimental conditions suggests that there is direct involvement of the network of hydrogen bonds borne by the secondary cyclodextrin face in the association process. In view of the potential use of the *tert*-butyldimethylsilyl cyclodextrins as calibration species for determining molecular weights, care should thus be paid to derivatize the secondary faces (alkylation or acylation) to avoid self-association or other aggregation phenomena.

Experimental Section

Synthesis: Microanalysis were performed by the Service de Microanalyses de l'Université Pierre et Marie Curie (Paris). Melting points were recorded on a Kofler Heizbank. ¹H NMR and ¹³C NMR spectra were recorded on an Bruker AM200SY spectrometer at room temperature. Chemical shifts are given in ppm with the protonated or ¹³C-labelled solvent as an internal reference (¹H NMR: CHCl₃ in CDCl₃, δ = 7.26; ¹³CDCl₃ in CDCl₃, δ = 76.9); coupling constants are given in Hz. Column chromatography was performed on Merck Silica Gel 60 (0.040–0.063 mm). The synthesis of

the 6^A,6^B,6^C,6^D,6^E,6^F,6^G-hepta-*O*-(*tert*-butyldimethylsilyloxy)- β -cyclodextrin (**1 β**), 2^A,2^B,2^C,2^D,2^E,2^F,2^G,3^A,3^B,3^C,3^D,3^E,3^F,3^G-tetradeca-*O*-benzyl-6^A,6^B,6^C,6^D,6^E,6^F,6^G-hepta-*O*-(*tert*-butyldimethylsilyloxy)- β -cyclodextrin (**5 β**), 2^A,2^B,2^C,2^D,2^E,2^F,2^G,3^A,3^B,3^C,3^D,3^E,3^F,3^G-tetradeca-*O*-benzyl- β -cyclodextrin (**6 β**), and 2^A,2^B,2^C,2^D,2^E,2^F,2^G,3^A,3^B,3^C,3^D,3^E,3^F,3^G,6^H-octadeca-*O*-benzyl- β -cyclodextrin (**6 γ**) have been previously reported.^[5a] 6^A,6^B,6^C,6^D,6^E,6^F-hexa-*O*-(*tert*-butyldimethylsilyloxy)- α -cyclodextrin (**1 α**)^[33] and 6^A,6^B,6^C,6^D,6^E,6^F,6^G,6^H-octa-*O*-(*tert*-butyldimethylsilyloxy)- γ -cyclodextrin (**1 γ**)^[33] were synthesized according to the method used in reference [5a]. The 2^A,2^B,2^C,2^D,2^E,2^F,2^G-hepta-*O*-methyl-6^A,6^B,6^C,6^D,6^E,6^F,6^G-hepta-*O*-(*tert*-butyldimethylsilyloxy)- β -cyclodextrin (**2 β**) and 2^A,2^B,2^C,2^D,2^E,2^F,2^G,3^A,3^B,3^C,3^D,3^E,3^F,3^G-tetradeca-*O*-methyl-6^A,6^B,6^C,6^D,6^E,6^F,6^G-hepta-*O*-(*tert*-butyldimethylsilyloxy)- β -cyclodextrin (**3 β**) were obtained as described in the literature^[5b] by using THF instead of DMF as a solvent. All compounds displayed satisfactory elemental analysis, melting points and spectroscopic features.

2^A,2^B,2^C,2^D,2^E,2^F,2^G-Hepta-*O*-benzyl-6^A,6^B,6^C,6^D,6^E,6^F,6^G-hepta-*O*-(*tert*-butyldimethylsilyloxy)- β -cyclodextrin (4 β**):** A mixture of **1 β** (1.16 g; 0.6 mmol), BaO (7.5 g; 49 mmol), Ba(OH)₂ (7.5 g; 43.9 mmol), benzyl bromide (6 cm³; 50.8 mmol), H₂O (0.1 cm³), and THF (60 cm³) was stirred over a week at room temperature. Concentrated NH₃ (30 cm³) was added and the mixture extracted with pentane. The organic phase was washed with HCl 1.2 M, then with saturated NaCl, and dried (Na₂SO₄). Final purification: column chromatography (silica gel, gradient elution with MeOH in CH₂Cl₂). The residue was recrystallized by slow evaporation of a mixture MeOH/pentane to give white crystals of **4 β** (0.727 g, 47%). M.p. 186 °C; ¹H NMR (200 MHz, CDCl₃, 25 °C, TMS) δ = 7.4 (m, 5H), 5.05 and 4.75 (AB, *J*_{AB} = 12 Hz, 2H), 4.95 (s, 1H), 4.8 (d, ³*J*(H,H) = 3 Hz, 1H), 4.05 (dd, ³*J*(H,H) = 9 Hz, ³*J*(H,H) = 9 Hz, 1H), 3.85 (d, ³*J*(H,H) = 10 Hz, 1H), 3.7–3.3 (m, 4H), 0.9 (s, 9H), 0.08 (s, 3H), 0.05 (s, 3H); ¹³C NMR (50.3 MHz, CDCl₃, 25 °C, TMS) δ = 137.7, 128.6, 128.2, 127.8, 101.2, 82.1, 79.1, 77.6, 76.9, 76.3, 73.9, 73.5, 71.7, 61.7, 25.9, 18.2, –5.1, –5.3; (C₁₉H₃₀O₅Si)_n (2565.8): calcd C 62.26, H 8.25; found C 62.49, H 8.23; TLC (SiO₂; CH₂Cl₂/Et₂O 85:15): *R*_f = 0.25.

Isotherm experiments: Compression isotherms were obtained with Millipore water subphase using a computer-controlled Lauda film balance. 50–100 μ L amount of the solutions of cyclodextrin derivatives in chloroform ([**1 α**] = 3.65 μ M; [**1 β**] = 2.89 μ M; [**1 γ**] = 3.44 μ M) or in a 1:1 chloroform/hexane mixture ([**6 β**] = 2.65 μ M; [**6 γ**] = 1.79 μ M) were spread on the aqueous surface and the solvent allowed to evaporate during 15 min. The compression was then performed at 0.1–1 $\text{Å}^2\text{s}^{-1}\text{molecule}^{-1}$ according to the experiments.

VPO experiments: Vapor pressure osmometry was performed with an Osmomat 070 [Gonotec, Berlin, (Germany)] in toluene at 45 °C. The apparatus was calibrated with monodisperse polystyrene standards of *M*_n = 2630, typically used for size exclusion chromatography (TSK standards, Tosoh Corp).

SEC experiments: Size exclusion chromatography was performed on a Waters system (Ultrastraygel columns).

NMR experiments: 5 mm NMR tubes were filled up with 0.5 mL of solution at the specified concentrations. For relaxation experiments, NMR tubes were submitted to freeze–thaw cycles under argon and high vacuum, and were finally sealed under vacuum. ¹H and ¹³C NMR spectra were acquired at 400.13 and 100.62 MHz, respectively, on a DRX Bruker spectrometer with standard pulse sequences at 294 ± 1 K. Chemical shifts are given in ppm related to the protonated solvent as internal reference (CHD₅ in C₆D₆: δ = 7.120; CHCl₃ in CDCl₃: δ = 7.210; CHD₂COCD₃ in CD₃COCD₃: δ = 2.020). The temperature was classically calibrated by measuring the separation between the two lines from a sample of glycol in [D₆]DMSO. Rotamer populations have been extracted from experimental ³*J*_{5,6i}^h (*i* = a or b) coupling constants by considering the three staggered conformers: GG (dihedral angles: O5–C5–C6–O6, 60°; C4–C5–C6–O6, 60°), GT (dihedral angles: O5–C5–C6–O6, 60°; C4–C5–C6–O6, 180°) and TG (dihedral angles: O5–C5–C6–O6, 180°; C4–C5–C6–O6, 60°), whose corresponding theoretical coupling constants ³*J*_{5,6i}^h are available in the literature.^[34] The respective populations *p*_{GG}, *p*_{GT}, *p*_{TG} are obtained by solving a system of linear equations [Eqs. (5), (6)]. Experimental heteronuclear proton–carbon NOE factors (NOEF) η_{exp} were determined from integration of ¹³C signals obtained from two different NMR experiments according to Equation (7), in which *I*_{sat} and *I*₀ respectively designates the

intensity of the ^{13}C NMR signals in the presence or in the absence of proton saturation. Simulated NOEF η_{sim} have been obtained from Equation (8), in which $J(\omega)$ is the spectral density function describing the motion of the dipolar coupled nuclei.

$${}^3J_{5,6i}^{\text{exp}} = P_{\text{GG}} {}^3J_{5,6i}^{\text{GG,th}} + P_{\text{TG}} {}^3J_{5,6i}^{\text{TG,th}} + P_{\text{GT}} {}^3J_{5,6i}^{\text{GT,th}} \quad (5)$$

$$1 = P_{\text{GG}} + P_{\text{TG}} + P_{\text{GT}} \quad (6)$$

$$\eta = \frac{I_{\text{sat}} - I_0}{I_0} \quad (7)$$

$$\eta = \frac{\gamma_{\text{H}}[6J(\omega_{\text{H}} + \omega_{\text{C}}) - J(\omega_{\text{H}} - \omega_{\text{C}})]}{\gamma_{\text{C}}[J(\omega_{\text{H}} - \omega_{\text{C}}) + 3J(\omega_{\text{C}}) + 6J(\omega_{\text{H}} + \omega_{\text{C}})]} \quad (8)$$

Two cases were considered for describing the molecular dynamics of the diverse species involved in the present study: i) a rigid body undergoing isotropic overall tumbling; ii) a rigid body undergoing anisotropic axially symmetrical overall tumbling. The corresponding spectral densities are given in Equations (9) and (10), in which $q_{ij} = 0.1 \gamma_{\text{H}}^2 \hbar^2 \tau_{ij}^{-6}$, $\tau_{\text{a}} = \tau_{\perp}$, $1/\tau_{\text{b}} = 5/(6\tau_{\perp}) + 1/(6\tau_{\parallel})$, $1/\tau_{\text{c}} = 1/(3\tau_{\perp}) + 2/(3\tau_{\parallel})$ and θ is the angle between the relaxation vector and the symmetry axis.^[35]

$$J_{\text{iso}} = q_{ij} \frac{\tau_{\text{c}}}{(1 + \omega^2 \tau_{\text{c}}^2)} \quad (9)$$

$$J_{\text{aniso}} = q_{ij} \left[0.25 \frac{(3 \cos^2 \theta - 1)^2 \tau_{\text{a}}}{(1 + \omega^2 \tau_{\text{a}}^2)} \right] + \left[\frac{3 \sin^2 \theta \cos^2 \theta \tau_{\text{b}}}{(1 + \omega^2 \tau_{\text{b}}^2)} \right] + \left[0.75 \frac{\sin^4 \theta \tau_{\text{c}}}{(1 + \omega^2 \tau_{\text{c}}^2)} \right] \quad (10)$$

In the case ii), the cartesian coordinates of the crystallographic β -cyclodextrin–ethanol complex structure^[36] were transformed into 1α structures with the Quanta[®] 4.0 commercial package (MSI). The two interacting units were positioned as displayed in Figure 8 with the plane containing anomeric oxygen atoms and the symmetry axis as reference plane and axis, respectively, for defining cyclodextrin orientation. For each carbon atom of the cyclodextrin backbone, the simulated NOEF value results from averaging over the seven corresponding θ values of the seven glucose units of the β -cyclodextrin.^[37] The mean standard deviation F between simulated η_{exp} and experimental η_{sim} NOEF has been calculated according to Equation (11).

$$F = \sqrt{\sum_i \left(\frac{\eta_{\text{exp}}(i) - \eta_{\text{sim}}(i)}{\eta_{\text{exp}}(i)} \right)^2} \quad (11)$$

Simulation of correlation times: The following viscosity^[38] has been used to simulate hydrodynamic data: $\eta_{294}(\text{benzene}) = 0.64 \text{ cp} = 0.64 \times 10^{-3} \text{ Pa s}^{-1}$. The correlation times have been calculated for different shapes:

- Sphere: The correlation time τ_{c} around any axis containing the sphere center as measured by NMR relaxation experiments is given by Equation (12).
- Right circular cylinder: Two correlation times describe the cylinder rotational motion: τ_{\parallel} (τ_{\perp}) for the rotation about the symmetry axis (about an inertial axis normal to the symmetry axis). τ_{\parallel} and τ_{\perp} are not independent and both can be calculated as a function of the aspect ratio $p = L/D$. Semiempirical equations [Eq. (13) with $\delta_{\text{perp}} = -0.662 + 0.917/p - 0.050/p^2$ and Eq. (14) with $A = 3.841$ and $\delta_{\text{para}} = 1.119 \times 10^{-4} + 0.6884/p - 0.2019/p^2$] are obtained for τ_{\perp} and τ_{\parallel} in the range $2 \leq p \leq 30$.^[39–41]

$$\tau_{\text{c}} = \frac{4\pi\eta R^3}{3kT} \quad (12)$$

$$1/(6\tau_{\perp}) = \frac{3kT(\ln p + \delta_{\text{perp}})}{\pi\eta L^3} \quad (13)$$

$$1/(6\tau_{\parallel}) = \frac{4kT}{A\pi\eta L D^2 (1 + \delta_{\text{para}})} \quad (14)$$

In view of the experimental errors, the agreement between experimental and semiempirical results,^[42] and between data contained in both refs. [40] and [42] led us to extrapolate Equations (13) and (14) up to $p = 1$. In fact, the authors of ref. [39] mention that these equations probably apply fairly well below $p = 2$.

Acknowledgements

Dr. S. Boileau is gratefully acknowledged for the access to toluene SEC measurements. L.J. and A.L. are indebted to the Ministère des Affaires Étrangères (Programme d'Actions Intégrées franco-belge TOURNESOL 1997) and to the CNRS (Coopération CNRS/CGRI-FNRS) for financial support. A.L. thanks the Belgian State (Services du Premier Ministre–Services fédéraux des Affaires scientifiques, programme PAI4/11) for financial support. Drs. M. Lahav and L. Leiserowitz are acknowledged for their kind hospitality and the CNRS for its corresponding grant (Coopération CNRS/MOSA Israel 1995).

- a) B. Alberts, D. Bray, J. Lewis, M. Raff, K. Roberts, J. D. Watson, *Molecular Biology of the Cell*, 3rd ed., Garland, New York, London, **1994**; b) C. Chotia, *Ann. Rev. Biochem.* **1984**, *53*, 537–572.
- a) A. Marsh, E. G. Nolen, K. M. Gardinier, J.-M. Lehn, *Tetrahedron Lett.* **1994**, 397–400; b) N. Kimizuka, S. Fujikawa, H. Kuwahara, T. Kunitake, A. Marsh, J.-M. Lehn, *J. Chem. Soc. Chem. Commun.* **1995**, 2103–2104; c) N. Branda, G. Kurz, J.-M. Lehn, *Chem. Commun.* **1996**, 2443–2444.
- A. P. Croft, R. A. Bartsch, *Tetrahedron*, **1983**, *39*, 1417–1474.
- C. R. Cantor, P. R. Schimmel, in *Biophysical Chemistry, Part II*, Freeman, New York, **1980**.
- a) L. Jullien, J. Canceill, L. Lacombe, J.-M. Lehn, *J. Chem. Soc. Perkin Trans. 2* **1994**, 989–1002, and references therein; b) K. Takeo, H. Mitoh, K. Uemura, *Carbohydr. Res.* **1989**, *187*, 203–221.
- Electrospray experiments suggest that 1β remains monomeric in a mixture of water and acetonitrile, see: M. Eddaoudi, A. W. Coleman, P. Prognon, P. Lopez-Mahia, *J. Chem. Soc. Perkin Trans. 2* **1996**, 955–959. Nevertheless, the latter result is difficult to analyze for extracting the extrapolated associative behavior in pure water, since specific solvation of 1β by acetonitrile is expected to occur in water–acetonitrile mixtures, even at low acetonitrile molar fractions.
- For side-on arrangement see: A. Laschewsky, *Adv. Mater.* **1989**, *1*, 392–395.
- G. L. Gaines, in *Insoluble monolayers at Liquid Gas Interfaces*, Interscience, Wiley, New York, **1966**.
- K. A. Connors, in *Binding Constants The Measurement of Molecular Complex Stability*, Wiley, New York, Chichester, Brisbane, Toronto, Singapore, **1987**.
- No splitting of signals that could appear under the assumption of a slow exchange regime has been observed in the course of the present study.
- By assuming the 1β solution to be perfect (no interaction between 1β molecules) and by considering a description that involves only two characteristic chemical shifts δ_1 and δ_2 , which correspond to the chemical shifts of 1β when 1β molecules are in 1) close proximity or 2) when they are infinitely diluted, respectively, the average chemical shift in a regime of fast exchange is given by considering that the probability of being in either state 1) or 2) is equal to the corresponding volume fractions [Eq. (15)]

$$\bar{\delta} = \delta_2 + \frac{4\pi}{3} N_{\text{A}} (\delta_1 - \delta_2) [(R + \lambda)^3 - R^3] [1\beta] \quad (15)$$

In Equation (15) N_{A} is the Avogadro number, R the radius of 1β under assumption of a spherical shape ($R \approx 1 \text{ nm}$; vide infra), and λ is a solvent-characteristic range for inducing chemical shifts in ^1H NMR. One can reasonably assume that the chemical shift is stabilized after addition of a solvation shell around the 1β molecules so as to give λ in the 0.5 nm range. The experimentally found dependence of the *tert*-butyl ^1H NMR chemical shift as a function of $[1\beta]_{\text{tot}}$ is indeed linear. Moreover, the extracted curve slope (20 ppm m^{-1}) eventually provides an estimate of $\delta_1 - \delta_2 \approx 6.5 \text{ ppm}$ that is in satisfactory agreement in sign and order of magnitude with the expected shielding effect from the benzene ring current.

- B. Hamelin, L. Jullien, C. Derouet, C. Hervé du Penhoat, P. Berthault, *J. Am. Chem. Soc.* **1998**, *120*, 8438–8447, and references therein.
- M. Hricovini, M. Guerrini, G. Torri, B. Casu, *Carbohydr. Res.* **1997**, *300*, 69–76.

- [14] The corresponding VPO experiments are not reliable at low concentration due to impurities in the solvents. Pure chloroform is unstable and known to contain hydrogen chloride, whereas THF contains water; this would affect the measurements in these solvents.
- [15] F. G. Stevens, *Biophys. J.* **1989**, *55*, 1155–1167.
- [16] Slowly is taken here as the timescale of elution: 1–10 min.
- [17] The group of A. Coleman has already extensively investigated the complexing properties of **1 β** at the air–water interface. For an example of ion complexation, see: M. Eddaoudi, A. Baszkin, H. Parrot-Lopez, M. M. Boissonade, A. W. Coleman, *Langmuir* **1995**, *11*, 13–15; for an example of complexation of neutral organic molecules, see: M. Eddaoudi, A. W. Coleman, A. Baszkin, *Supramol. Chem.* **1997**, *8*, 177–180.
- [18] Y. Kawabata, M. Matsumoto, M. Tanaka, H. Takahashi, Y. Irinatsu, S. Tamura, W. Tagaki, H. Nakahara, K. Fukuda, *Chem. Lett.* **1986**, 1933–1934.
- [19] S. Taneva, K. Ariga, W. Tagaki, Y. Okahata, *J. Coll. Interface Sci.* **1989**, *131*, 561–566.
- [20] H. Parrot-Lopez, C.-C. Ling, P. Zhang, A. Baszkin, G. Albrecht, C. De Rango, A. Coleman, *J. Am. Chem. Soc.* **1992**, *114*, 5479–5481.
- [21] M. H. Greenhall, P. Lukes, R. Katakay, N. E. Agbor, J. P. S. Badyal, J. Yarwood, D. Parker, M. C. Petty, *Langmuir* **1995**, *11*, 3997–4000.
- [22] A. Kaselouri, M. Munoz, H. Parrot-Lopez, A. W. Coleman, *Pol. J. Chem.* **1993**, *67*, 1981–1985.
- [23] I. Nicolis, A. W. Coleman, P. Charpin, F. Villain, P. Zhang, C. C. Ling, C. De Rango, *J. Am. Chem. Soc.* **1993**, *115*, 11596–11597.
- [24] a) H. Diep-Quang, K. Ueberreiter, *Colloid Polymer Sci.* **1980**, *258*, 1055–1061; b) M. van der Auweraer, C. Catry, L. F. Chi, O. Karthaus, W. Knoll, H. Ringsdorf, M. Sawodny, C. Urban, *Thin Solid Films* **1992**, *210/211*, 39–41; c) M. N. G. de Mul, J. A. Mann, Jr., *Langmuir* **1994**, *10*, 2311–2316; d) J. Fang, M. Dennin, C. M. Knobler, Yu. K. Godovsky, N. N. Makarova, H. Yokoyama, *J. Phys. Chem. B* **1997**, *101*, 3147–3154; e) J. A. Schröter, R. Plehnert, C. Tschierske, *Langmuir* **1997**, *13*, 796–800.
- [25] a) S. Alexandre, A. W. Coleman, A. Kasselouri, J. M. Valleton, *Thin Solid Films* **1996**, *284/285*, 735–768; b) J. Majewski, R. Edgar, R. Popovitz-Biro, K. Kjaer, W. Bouwman, J. Als-Nielsen, M. Lahav, L. Leiserowitz, *Angew. Chem.* **1995**, *107*, 707–711; *Angew. Chem. Int. Ed. Engl.* **1995**, *34*, 649–652.
- [26] In particular, the agreement suggests that the lifetime of the solvent molecules on cyclodextrin surfaces exceeds several nanoseconds. Otherwise, slip boundary conditions would apply and the friction coefficient for rotation would be zero. See for instance the ref. [4].
- [27] If one takes a larger diameter D as a mean to increase the friction at the ends of the cylinder, the equilibrium distance d between **1 β** interacting units is strongly reduced. For instance with $D = 2.2$ nm, one obtains a minimum of F at $L = 3.3$ nm that gives $d = 0.7$ nm.
- [28] The different behaviour of **3 β** can be explained by the absence of hydroxyl groups on the secondary face of the cyclodextrin. When they exist, the latter hydroxyl groups form an intramolecular network of hydrogen bonds that gives its rigidity to the cyclodextrin skeleton, see for instance: K. B. Lipkowitz, K. Green, J. Yang, *Chirality* **1992**, *4*, 205–215; K. B. Lipkowitz, *J. Org. Chem.* **1991**, *56*, 6357–6367. Consequently, **1 β** and **2 β** should exhibit similar cyclodextrin backbones and thus close arrangement of 6-glucose substituents whereas the primary face of **3 β** could be arranged in a different way.
- [29] As already underlined, we suppose that the hydroxyl group at the C3 glucose position is engaged in an intramolecular hydrogen bond with the oxygen at the C2 position of the neighbouring glucose unit. Consequently, we do not take into account the corresponding hydroxyl groups for discussing the dimerization process.
- [30] This value compares well with other systems with hydrogen bond interactions. See for instance: H.-J. Schneider, *Angew. Chem.* **1991**, *103*, 1419–1439; *Angew. Chem. Int. Ed. Engl.* **1991**, *30*, 1417–1436.
- [31] a) J. S. Boger, R. J. Corcoran, J. M. Lehn, *Helv. Chim. Acta.* **1978**, *61*, 2190–2218; b) P. Ellwood, C. M. Spencer, N. Spencer, J. F. Stoddart, R. Zarzycki, *J. Inclusion Phenom. Mol. Recogn.* **1992**, *12*, 121–150.
- [32] J. Israelachvili, in *Intermolecular and Surface Forces*, 2nd ed., Academic Press, London, San Diego, New York, Boston, Sydney, Tokyo, Toronto, **1991**.
- [33] P. Fügedi, *Carbohydr. Res.* **1989**, *192*, 366–369.
- [34] C. A. G. Haasnoot, *Tetrahedron* **1980**, *36*, 2783–2792.
- [35] D. E. Woessner, *J. Chem. Phys.* **1962**, *37*, 647–654.
- [36] T. Steiner, S. A. Mason, W. Saenger, *J. Am. Chem. Soc.* **1991**, *113*, 5676–5687.
- [37] To calculate the simulated NOEF, the average over the seven glucose residues present in the β -cyclodextrin backbone can be performed either by averaging the θ angles, the respective spectral density functions, or the NOEF. Whichever the way which is chosen, the averaging yields essentially the same results at the precision of the present experimental determination.
- [38] *Handbook of Chemistry and Physics*, 61st ed., CRC, Boca Raton, **1980–1981**.
- [39] W. Eimer, J. R. Williamson, S. G. Boxer, R. Pecora, *Biochemistry* **1990**, *29*, 799–811.
- [40] M. M. Tirado, C. L. Martinez, J. Garcia De La Torre, *J. Chem. Phys.* **1984**, *81*, 2047–2052.
- [41] M. M. Tirado, J. Garcia De La Torre, *J. Chem. Phys.* **1980**, *73*, 1986–1993.
- [42] E. Swanson, C. Teller, D. C. De Haën, *J. Chem. Phys.* **1978**, *68*, 5097–5102.

Received: June 4, 1998 [F1189]